



## Ultrasonic and spectroscopic investigations of molecular interactions in binary mixture of PEG-400 and DMSO at different temperatures

MONIKA DHIMAN<sup>1</sup>, ARUN UPMANYU<sup>1\*</sup>, DEVINDER PAL SINGH<sup>2</sup>  
and KAILASH CHANDRA JUGLAN<sup>3</sup>

<sup>1</sup>Chitkara University Institute of Engineering and Technology, Chitkara University, Punjab, 140401, India, <sup>2</sup>Acoustics Research Center, Mississauga, L5A 1Y7, Ontario, Canada and

<sup>3</sup>Department of Physics, Lovely Faculty of Technology and Sciences, Lovely Professional University, Punjab, India

(Received 7 December 2023, revised 22 January, accepted 2 June 2024)

**Abstract:** In the present study, the ultrasonic velocity and density data for the binary mixture of polyethylene glycol (PEG)-400 and dimethyl sulfoxide (DMSO), at various concentrations and different temperatures ( $T$ , 288.15, 298.15 and 308.15 K), have been measured and further applied to determine several physical parameters such as adiabatic and isothermal compressibility, intermolecular free length, internal pressure and free volume. The excess values of these parameters have also been computed and fitted with the Redlich-Kister (R-K) polynomial equation. The nature, type, and strength of intermolecular interactions present within the PEG-400 + DMSO mixture have been explained based on the sign and magnitude of excess values. Furthermore, partial molar volumes, excess partial molar volumes, apparent molar volumes and apparent molar volumes at infinite dilution have also been determined to investigate the solute–solvent interactions. Various mixing rules such as the ideal mixing rule ( $U_{im}$ ), Nomoto relation ( $U_N$ ), impedance dependence relation ( $U_Z$ ), Junjie relation ( $U_J$ ), van Deal–Vangeel relation ( $U_V$ ) and collision factor theory ( $U_{CFT}$ ) are employed to compute the ultrasonic velocity and compared with the experimental one. Among these relations, the Nomoto and Junjie relations are found to be most suitable for the given mixture. In addition to it, the present system has also been examined using Fourier transform infra-red (FTIR) and UV–Vis spectroscopic techniques. The change in intensity and shift in peak position in the FTIR and UV–Vis spectra of the PEG-400 + DMSO mixture are used to confirm the intermolecular hydrogen bonding in the given system.

**Keywords:** research development; industry; sustainable development; polyethylene glycol; Fourier transform infra-red (FTIR); UV–Vis.

\*Corresponding author. E-mail: arun.upmanyu@chitkara.edu.in  
<https://doi.org/10.2298/JSC231207058D>

## INTRODUCTION

In recent years, several researchers have contributed to synthesizing and characterizing significant industrial materials and tuning them to specific applications.<sup>1–5</sup> In such chemical synthesis, the emission of sulphur dioxide ( $\text{SO}_2$ ) is a serious concern that affects the health and environmental sectors.<sup>3–5</sup> Therefore, various processes/techniques have been developed over time to remove  $\text{SO}_2$  from industrial products, a process called desulphurisation.<sup>6–8</sup> Dimethyl sulfoxide (DMSO) is a widely used organic solvent for removing  $\text{SO}_2$  due to its high solubility for sulphur-containing compounds. However, the high freezing point (18 °C) of DMSO causes problems to use it in the low-temperature range. Adding another biocompatible polyethylene glycol (PEG)-400 into DMSO will overcome this limitation. The other advantages of the PEG-400 + DMSO mixture are its relatively low toxicity and better solubility than virgin DMSO. Furthermore, it can be easily recovered and reused in chemical processes.

A comprehensive review of the literature<sup>6,9–12</sup> reveals that most of the investigations into the PEG-400 and DMSO systems are made to understand their behaviour towards desulphurisation, whereas only limited work is available to explore the nature and strength of inter- and intra-molecular interactions prevalent within the system based on the ultrasonic velocity, density and viscosity. Zhang *et al.*<sup>6</sup> also measured the density of the PEG-400 + DMSO mixture at different concentrations and temperatures. To compare the reported density data with the present data at mutual temperatures (298.15 and 308.15 K), we have generated the fitting equation for density measured in this work:

$$d^* = Y_0 + A \exp(R_0 X_1) \quad (1)$$

where  $Y_0$ ,  $A$  and  $R_0$  are the arbitrary constants and their values at: a)  $T = 298.15$  K are:  $Y_0 = 1.1216$ ,  $A = -0.0244$  and  $R_0 = -4.8551$ ; b)  $T = 308.15$  K are:  $Y_0 = 1.1139$ ,  $A = -0.0258$  and  $R_0 = -4.0890$ .

Thereafter, Eq. (1) was used to compute the density ( $d^*$ ) at the same mole fractions as reported in a research paper by Zhang *et al.*<sup>6</sup> The correlation of measured density and the one reported in literature<sup>6</sup> along with the absolute average percentage deviation (AAPD) at 298.15 and 308.15 K are given in Table S-I (Supplementary material to this paper). The perusal of Table S-I indicates that the AAPD is 0.1550 and 0.1488 at 298.15 and 308.15 K, respectively. For a better understanding, the density data obtained in the present study and literature,<sup>6</sup> along with the fitting line, are given in Figs. S-1 and S-2 (Supplementary material). Additionally, the density values of current measurement (using Eq. (1)) and literature<sup>6</sup> at the same mole fractions are presented in Figs. S4 and S-5 (Supplementary material). The probable reason for the deviation can be: *i*) Zhang *et al.*<sup>6</sup> performed the pre-processing (drying over molecular sieves (type 4A) and decompression filtration by vacuum pump), before density measurement of the

materials, whereas in the present work, these materials are used as such without any further purification; *ii)* additionally, we have measured the density using more sophisticated DSA 5000 M interferometer, with the density accuracy of  $0.000001\text{ g cm}^{-3}$ ; Zhang *et al.*<sup>6</sup> measured density using bicapillary pycnometer.

Moreover, there are several techniques such as infrared (IR) spectroscopy, nuclear magnetic resonance (NMR) spectroscopy, UV–Vis spectroscopy, X-ray crystallography, surface plasmon resonance (SPR), isothermal titration calorimetry (ITC), fluorescence resonance energy transfer (FRET) technique, ultrasonic, volumetric and refractometric techniques are available to investigate different types of molecular interactions in the solid/liquid systems. A literature survey<sup>13–18</sup> reveals that the ultrasonic technique is widely accepted to study molecular interactions for liquid systems due to its unique features like its non-destructive nature, real-time monitoring, versatility, high sensitivity and non-invasiveness. The ultrasonic technique involves measuring the speed and attenuation of ultrasonic waves as they pass through a liquid system. The speed of the ultrasonic wave is affected by the density and compressibility of the liquid mixture, while the attenuation is affected by the viscosity and molecular interactions present in the system. By analysing the changes in speed and attenuation of the ultrasonic waves, it is possible to obtain information about the nature, type, and strength of interactions among the constituent molecules of the mixture. The speed of sound in conjunction with density can be further employed to calculate several important thermodynamical parameters such as acoustic impedance, adiabatic compressibility, intermolecular free length, internal pressure, free volume, *etc.*, which are generally difficult to determine experimentally. The concentration and temperature dependence of these parameters also provide useful information about inter and intra-molecular interactions, prevalent in the system. Other useful techniques to study the molecular interactions in liquid systems are FTIR, UV and NMR spectroscopy.<sup>19–21</sup> These techniques rely on the interaction of electromagnetic radiation with the molecules in a sample. The absorption, emission, or scattering of electromagnetic radiation by the sample is measured. The obtained data provides information about the sample's molecular structure and interactions. At present, ultrasonic and spectroscopic techniques are regularly used to investigate the molecular interactions in organic liquids, polymers, polymer blends, ionic liquids and liquid crystals.<sup>22–24</sup>

In the present work, ultrasonic velocity and density values are measured for PEG-400 + DMSO at different mole fractions and temperatures (288.15, 298.15 and 308.15 K). The measured data are used to compute several important thermodynamical parameters such as adiabatic and isothermal compressibility, intermolecular free length, internal pressure, free volume and their excess values. FTIR and UV–Vis spectroscopic investigation has also been taken to explore the molecular interactions in the system under study. The variations in sign and mag-

nitude of excess parameters, with changes in concentration and temperature, have been used to complement/supplement the information obtained *via* other investigative techniques about the nature, type, and strength of molecular interactions prevalent in the system under study.

## EXPERIMENTAL

### Materials

Polyethylene glycol (PEG) and DMSO with molar masses of 400 and 78.14 g·mol<sup>-1</sup>, respectively, and purity ≥ 99% were acquired from Loba Chemie Pvt. Ltd., India. The chemicals were used without any further purification for the measurement of ultrasonic velocity (*U*) and density (*d*).

### Measurement procedure of ultrasonic velocity (*U*) and density (*d*)

The ultrasonic velocity (*U*) and density (*d*) of the pure PEG-400, DMSO and their mixture at different mole fractions were measured at the three different temperatures (*T*, 288.15, 298.15 and 308.15 K) using Anton Paar DSA 5000M densimeter which worked at 3 MHZ. The inbuilt Peltier-thermostat of the densimeter controlled the temperature automatically and the working temperature was estimated accurately up to ±0.01 K. The *U* and *d* were measured by infusing the sample with a syringe inside the instrument. The instrument can measure density with an accuracy of 0.000001 g cm<sup>-3</sup> and ultrasonic velocity with an accuracy of 0.01 m s<sup>-1</sup>. For density measurement, the apparatus was calibrated with doubly distilled degassed water, and with dry air at atmospheric pressure. The repeatability is obtained with triplicate measurements on the same sample maintained inside the densimeter at a constant temperature at different times during the course of present measurements. The density and speed of sound measurements both had experimental uncertainties below 0.0005 g·m<sup>-3</sup> and 1.0 m·s<sup>-1</sup>, respectively. Binary mixtures were prepared by mass percents, using an analytical balance with a precision of 0.0001 g (Denver Instrument APX-200). The mole fraction of each mixture was obtained with an accuracy of 0.0001 from the measured masses of the components. The measured values of *U* and *d* of pure components had been compared with literature data and are reported in Table I. The contents of Table I indicates that the percentage deviation between experimental and literature values of density and ultrasonic velocity for PEG-400 and DMSO is less than 0.3 % at all temperatures. The comparisons between experimental and literature densities and ultrasonic velocity are presented in Fig. 1a–d.

TABLE I. Experimental and literature values of ultrasonic velocity (*U*) and density (*d*) of pure PEG-400 and DMSO; the standard uncertainties (*u*) are *u*(*T*) = 0.01 K, *u*(*d*) = 0.5 kg m<sup>-3</sup>, *u*(*U*) = 1.0 m s<sup>-1</sup>

Com- ponent	<i>T</i> / K	<i>U</i> / m s <sup>-1</sup>		Modulus of deviation, %	<i>d</i> / g cm <sup>-3</sup>		Modulus of deviation, %
		Exp.	Lit.		Exp.	Lit.	
PEG-400	288.15	1629.30	—		1.13031	1.13126 <sup>25</sup>	0.084
	298.15	1595.16	1592.8 <sup>26</sup>	0.146	1.12199	1.1226 <sup>6</sup>	0.060
		1595.03 <sup>27</sup>	0.008		1.12225 <sup>25</sup>		0.023
		1593.01 <sup>28</sup>	0.135		1.12239 <sup>26</sup>		0.036
		1593.20 <sup>29</sup>	0.123		1.122308 <sup>27</sup>		0.028
					1.12230 <sup>28</sup>		0.028
308.15	1561.90	1558.9 <sup>30</sup>	—	0.190	1.11373	1.1139 <sup>6</sup>	0.021
		1564.4 <sup>26</sup>	—	0.162	—	1.1128 <sup>30</sup>	0.081

TABLE I. Continued

Com- ponent	<i>T</i> / K	<i>U</i> / m s <sup>-1</sup>		Modulus of deviation, %	<i>d</i> / g cm <sup>-3</sup>		Modulus of deviation, %	
		Exp.	Lit.		Exp.	Lit.		
DMSO	288.15	1524.25	—	0.020 0.153 0.186 — 0.193 0.356 0.062 0.338 0.412 0.336 0.308 0.210 0.336 0.392 0.385 0.357 0.337 0.361	1.11433 <sup>26</sup>	0.054	0.153 0.103 0.104 — 1.0958 <sup>6</sup> 1.0952 <sup>32</sup> 1.0957 <sup>19</sup> 1.0954 <sup>35</sup> 1.09729 <sup>33</sup> 1.095387 <sup>34</sup> 1.09537 <sup>39</sup> 1.09562 <sup>41</sup> 1.09537 <sup>43</sup> 1.09527 <sup>45</sup> 1.08070 <sup>46</sup> 1.0852 <sup>32</sup> 1.08548 <sup>10</sup> 1.0857 <sup>19</sup> 1.085348 <sup>34</sup> 1.08550 <sup>47</sup> 1.0856 <sup>48</sup> 1.0839 <sup>6</sup>	0.013 0.045 0.000 0.026 0.144 0.030 0.032 0.009 0.032 0.041 0.598 0.181 0.158 0.136 0.170 0.156 0.143 0.304
		1490.12	1493 <sup>31</sup>					
		1484.8 <sup>32</sup>	—					
		1489.2 <sup>33</sup>	—					
		1485.10 <sup>34</sup>	—					
		1484 <sup>36</sup>	—					
		1485.12 <sup>37</sup>	—					
		1485.5 <sup>38</sup>	—					
		1487 <sup>40</sup>	—					
		1485.12 <sup>42</sup>	—					
		1484.29 <sup>44</sup>	—					
		1456.54	1450.9 <sup>32</sup>					
		1451.3 <sup>34</sup>	—					
		1451.6 <sup>39</sup>	—					
		1451.28 <sup>34</sup>	—					

#### FTIR and UV-Vis spectroscopy

The FTIR spectrum for the mixture under study was recorded on sophisticated FTIR (Bruker, model Eco AR Alpha II) equipped with Opus software. The spectrometer possessed auto-align energy optimization, dynamically aligned with and RockSolid™ cube corner interferometer and temperature-controlled DLaTGS-detector. Data were recorded in the spectral range of 400–4000 cm<sup>-1</sup> at 4 cm<sup>-1</sup> spectral resolution with standard KBr beam splitter possessing precision and accuracy of 0.05 cm<sup>-1</sup> at 1576 cm<sup>-1</sup> and <0.0006 cm<sup>-1</sup> at 1576 cm<sup>-1</sup>. A baseline correction was made for the spectra recorded in the air. For each measurement 10 µL a solution was used with sample layer thickness typically less than 2 µm. All these measurements were performed at room temperature and atmospheric pressure.

The UV-Vis spectrum for the mixture was recorded on Systronics (India) PC-based double beam UV-Vis spectrophotometer-2202. The spectrophotometer was equipped with modified Czerny-Turner monochromator geometry for better aberration correction, holographic diffraction grating with 1200 lines/mm blazed at 250 nm, and advanced beam technology with PC-controlled settings. The apparatus operates in the wavelength range from 200 to 1100 nm at a resolution of 0.1 nm with an accuracy of ±0.5 nm. In the present case, DMSO is used to make the baseline correction for the spectra.

#### Theoretical formulation

The experimentally measured data for *U* and *d* have been used to compute some physical parameters such as adiabatic compressibility (*K<sub>s</sub>*), isothermal compressibility (*K<sub>T</sub>*), inter-

molecular free length ( $L_f$ ), free volume ( $V_f$ ), and internal pressure ( $P_i$ ) by employing following standard formulations as reported in the literature:<sup>13</sup>

$$K_s = \frac{1}{U^2 d} \quad (2)$$

$$K_T = \frac{1.71 \times 10^{-3}}{T^{4/9} U^2 d^{4/3}} \quad (3)$$

$$L_f = \frac{2V_a}{Y_S} \quad (4)$$

where  $Y_S = (36\pi N V_0^2)^{1/3}$  is the molar surface area,  $N$  is Avogadro's number, and  $V_0 = V - V_a$ , where  $V$  is the molar volume,  $V_a$  is the available volume at any given temperature, and  $V_0$  is the molar volume of liquid at absolute zero temperature.

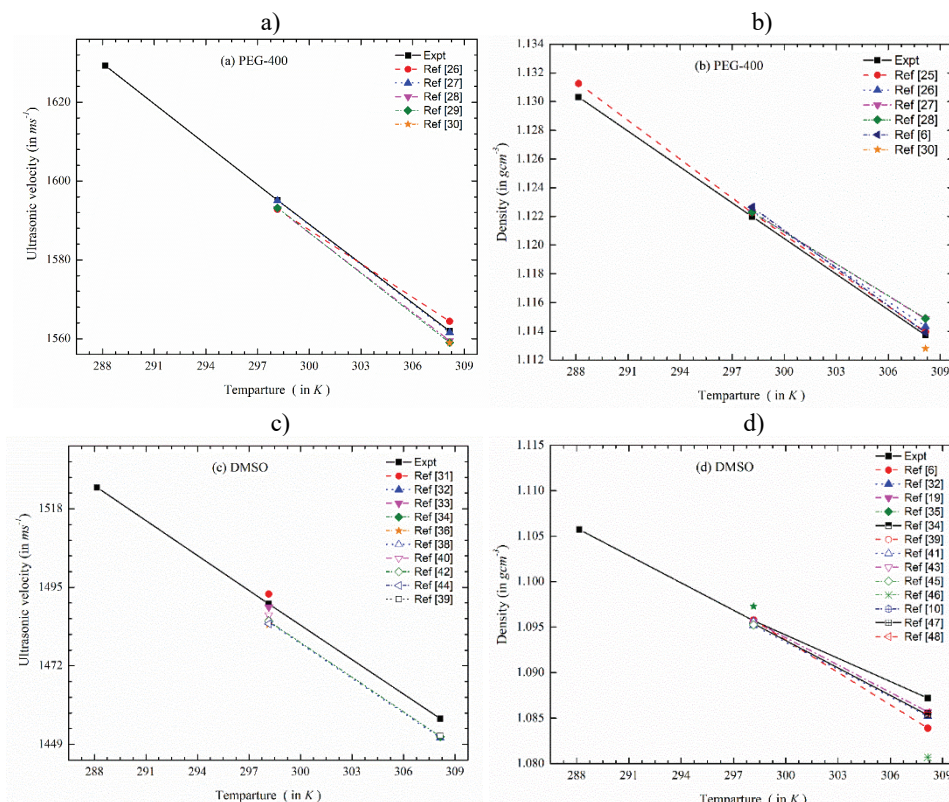


Fig. 1. The plot of experimental and literature values: a) of ultrasonic velocity of PEG-400 at 288.15, 298.15 and 308.15 K; b) of density of PEG-400 at 288.15, 298.15 and 308.15 K; c) for the ultrasonic velocity of DMSO at 288.15, 298.15 and 308.15 K; d) values for the density of DMSO at 288.15, 298.15 and 308.15 K. The solid and dotted lines are a guide for the eye.

The internal pressure ( $P_i$ ) is a measure of the strength of forces between the molecules and is obtained by using the following relation:

$$P_i = \frac{T\alpha}{K_T} \quad (5)$$

where  $T$  is temperature,  $K_T$  is isothermal compressibility, and volume expansivity ( $\alpha$ ) is given by  $\alpha = (0.0191 \times K_T)^{1/4}$ .

Another important parameter free volume ( $V_f$ ), which is the average volume of free space between the two neighbouring molecules is given below:

$$V_f = \frac{RT}{P + P_i} \quad (6)$$

where  $P$  is external pressure, which is negligible as compared to internal pressure ( $P_i$ ),  $R$  is universal gas constant, and  $T$  is temperature.

The theoretical evaluation of ultrasonic velocity ( $U$ ) has been done using various mixing rules *viz.*, ideal mixing rule ( $U_{im}$ ), Nomoto relation ( $U_N$ ), impedance dependence relation ( $U_Z$ ), Junjie relation ( $U_J$ ), Van Deal-Vangeel relation ( $U_V$ ), and collision factor theory ( $U_{CFT}$ ). The mathematical formulations for these relations are given below:<sup>13</sup>

The ideal mixing relation ( $U_{im}$ ) uses the speed of sound of pure components along with mole fraction to predict the ultrasonic velocity of the mixture, as:

$$U_{IM} = \sum_i^2 X_i U_i \quad (7)$$

where  $X_i$  and  $U_i$  ( $i = 1, 2$ ) are the mole fraction and sound velocity of pure components, respectively.

Nomoto relation ( $U_N$ ) based on the assumption of no volume change on mixing, is given as:

$$U_N = \left( \frac{X_1 R_1 + X_2 R_2}{X_1 V_1 + X_2 V_2} \right)^3 \quad (8)$$

where  $V_1$  and  $V_2$  are the molar volumes and  $R_1$  and  $R_2$  are the molar sound velocity values of the pure components in the binary mixture.

The standard form of impedance dependence relation ( $U_Z$ ) to predict ultrasonic velocity is:

$$U_Z = \frac{X_1 Z_1 + X_2 Z_2}{X_1 d_1 + X_2 d_2} \quad (9)$$

where  $X_1$ ,  $X_2$ ,  $Z_1$ ,  $Z_2$  and  $d_1$ ,  $d_2$  are, respectively, the mole fraction, acoustic impedance, and density values of pure components in a binary mixture.

Junjie relation ( $U_J$ ) predicts ultrasonic velocity using mole fractions  $X_1$  and  $X_2$ , molar masses  $M_1$  and  $M_2$ , molar volumes  $V_1$  and  $V_2$ , density  $d_1$ , and  $d_2$  and ultrasonic speed  $U_1$  and  $U_2$  of pure components:<sup>49</sup>

$$U_J = \frac{X_1 V_1 + X_2 V_2}{\sqrt{(X_1 M_1 + X_2 M_2)(X_1 V_1 / (d_1 U_1^2)) + X_2 V_2 / (d_2 U_2^2)}} \quad (10)$$

Van Deal and Vangeel ( $U_V$ ) modified the ideal mixing relation using molar weight  $M_1$  and  $M_2$  of pure components;<sup>13</sup>

$$U_V = \frac{1}{\sqrt{(X_1 M_1 + X_2 M_2)(X_1 / (d_1 U_1^2)) + X_2 / (d_2 U_2^2)}} \quad (11)$$

The collision factor theory ( $U_{CFT}$ ) is based on the concept of collisions taking place amongst liquid molecules and the free space available between them. It provides an expression for the calculation of ultrasonic velocities in a binary mixture, as given below:<sup>13</sup>

$$U_{CFT} = U_\infty (X_1 S_1 + X_2 S_2) \frac{X_1 B_1 + X_2 B_2}{V} \quad (12)$$

where  $U_\infty$  is the limiting value of sound velocity for liquids, which is taken as 1600 m s<sup>-1</sup>.  $S_1$  and  $S_2$  are collision factors.  $B_1$  and  $B_2$  are geometrical volumes per mole of solute and solvent, respectively.

## RESULTS AND DISCUSSION

### *Acoustical parameters and molecular interactions*

The experimentally measured ultrasonic velocity ( $U$ ) and density ( $d$ ) data for PEG-400 + DMSO binary mixture at various concentrations and temperatures are reported in Table II. Therein, the obtained results are presented as a function of the mole fraction ( $X_1$ ) of PEG-400 at different temperatures (288.15, 298.15 and 308.15 K).

TABLE II. Measured values of ultrasonic velocity ( $U$ ) and density ( $d$ ) of PEG-400 ( $X_1$ ) + DMSO ( $X_2$ ) at different temperatures

$X_1$	288.15 K		298.15 K		308.15 K	
	$U$ / m s <sup>-1</sup>	$d$ / g cm <sup>-3</sup>	$U$ / m s <sup>-1</sup>	$d$ / g cm <sup>-3</sup>	$U$ / m s <sup>-1</sup>	$d$ / g cm <sup>-3</sup>
0	1524.25	1.10574	1490.12	1.09572	1456.54	1.08720
0.0477	1564.03	1.11383	1522.6	1.10408	1489.42	1.09452
0.0790	1569.29	1.11716	1534.37	1.10604	1497.3	1.09549
0.1178	1574.43	1.11877	1547.78	1.10785	1513.44	1.09787
0.1668	1587.41	1.12024	1559.49	1.10936	1529.19	1.09934
0.2310	1598.23	1.12464	1567.88	1.11288	1539.9	1.10375
0.3185	1612.76	1.12614	1579.28	1.11712	1548.13	1.10771
0.4448	1618.22	1.12792	1583.57	1.11870	1550.07	1.11007
0.5516	1621.16	1.12855	1586.64	1.11957	1553.20	1.11104
0.6431	1623.25	1.12900	1588.84	1.12019	1555.44	1.11173
0.8278	1626.71	1.12975	1592.45	1.12122	1559.13	1.11287
1	1629.30	1.13031	1595.16	1.12199	1561.9	1.11373

Using the experimentally measured  $U$  and  $d$  values, some acoustical and thermodynamical parameters, *viz.*,  $K_s$ ,  $K_T$ ,  $L_f$ ,  $V_f$  and  $P_i$ , have been determined. These parameters are reported in Table III. Several researchers have pointed out that acoustical and thermodynamical parameters are important tools to explore the nature and strength of molecular interactions in a liquid system.<sup>50–52</sup> Keeping this in view, we have calculated the excess values of these acoustical and thermodynamical parameters using a standard relation as given below:

$$A^{\text{Excess}} = A^{\text{Exp}} - (A_1 X_1 + A_2 X_2) \quad (13)$$

where  $A$  represents  $K_s$ ,  $K_T$ ,  $L_f$ ,  $V_f$  and  $P_i$ .  $A^{\text{Excess}}$  and  $A^{\text{Exp}}$  are the excess and experimental values of  $A$ .  $X_1$  and  $X_2$  are the mole fractions of the solute and the solvent, respectively.

The excess values of all these parameters as a function of the mole fraction ( $X_1$ ) of PEG-400 are plotted in Figs. 2–6 at different temperatures. These excess values are also fitted with Redlich–Kister (R–K)<sup>11</sup> type polynomial equation given below:

$$\Delta Y = X_1 X_2 \sum_{K=1}^n A_K (2X_1 - 1)^{(K-1)} \quad (14)$$

where  $\Delta Y$  is the excess parameter to be fitted with the R–K polynomial equation, and  $A_K$  is the fitting parameter. The number of fitting parameters is optimized by using  $F$ -test.<sup>53</sup> The standard deviations ( $\sigma$ ) are computed using the relation:

$$\sigma(\Delta Y) = \sqrt{\frac{\sum(\Delta Y_{\text{Exp}} - \Delta Y_{\text{Cal}})^2}{N-n}} \quad (15)$$

where  $N$  is the total number of mole fractions and  $n$  is the number of fitting parameters.  $\Delta Y_{\text{exp}}$  and  $\Delta Y_{\text{Cal}}$  are the experimental and calculated values of excess parameters. The computed values of R–K coefficients and  $\sigma$  are reported in Table IV.

TABLE III. Acoustical parameters, *viz.*, free volume ( $V_f$ ), adiabatic compressibility ( $K_s$ ), isothermal compressibility ( $K_T$ ), intermolecular free length ( $L_f$ ) and internal pressure ( $P_i$ ) for PEG-400 + DMSO at different temperatures; the standard uncertainties ( $u$ ) are  $u(T) = 0.01$  K,  $u(d) = 0.5$  kg m<sup>-3</sup>,  $u(U) = 1.0$  m s<sup>-1</sup>

$X_1$	$V_f \times 10^6 / \text{m}^3 \text{ mol}^{-1}$	$K_s \times 10^{-10} / \text{Pa}^{-1}$	$K_T \times 10^{-10} / \text{Pa}^{-1}$	$L_f / \text{pm}$	$P_i / \text{MPa}$
$T = 288.15 \text{ K}$					
0	4.327±0.004	3.893±0.005	5.194±0.007	39.84±0.042	553.7±0.006
0.0477	4.133±0.004	3.670±0.005	4.886±0.007	38.69±0.035	579.7±0.006
0.0790	4.100±0.004	3.635±0.005	4.834±0.006	38.50±0.034	584.3±0.006
0.1178	4.074±0.004	3.606±0.005	4.793±0.006	38.35±0.034	588.1±0.006
0.1668	4.019±0.004	3.543±0.005	4.707±0.006	38.01±0.032	596.1±0.006
0.2310	3.962±0.004	3.481±0.005	4.619±0.006	37.68±0.030	604.6±0.006
0.3185	3.904±0.004	3.414±0.004	4.528±0.006	37.31±0.029	613.7±0.006
0.4448	3.878±0.003	3.386±0.004	4.488±0.006	37.16±0.028	617.8±0.006
0.5516	3.865±0.003	3.372±0.004	4.468±0.006	37.08±0.028	619.8±0.006
0.6431	3.856±0.003	3.361±0.004	4.454±0.006	37.02±0.027	621.3±0.006
0.8278	3.841±0.003	3.345±0.004	4.432±0.006	36.93±0.027	623.7±0.006
1	3.830±0.003	3.333±0.004	4.415±0.006	36.86±0.027	625.5±0.006
$T = 298.15 \text{ K}$					
0	4.466±0.004	4.110±0.006	5.418±0.008	41.70±0.050	555.0±0.006
0.0477	4.291±0.004	3.907±0.005	5.137±0.007	40.65±0.043	577.6±0.006
0.0790	4.235±0.004	3.840±0.005	5.047±0.007	40.31±0.041	585.4±0.006
0.1178	4.173±0.004	3.768±0.005	4.949±0.007	39.93±0.039	594.0±0.006

TABLE III. Continued

$X_1$	$V_f \times 10^6 / \text{m}^3 \text{ mol}^{-1}$	$K_s \times 10^{-10} / \text{Pa}^{-1}$	$K_T \times 10^{-10} / \text{Pa}^{-1}$	$L_f / \text{pm}$	$P_i / \text{MPa}$
$T = 298.15 \text{ K}$					
0.1668	4.120±0.004	3.706±0.005	4.866±0.007	39.60±0.037	601.6±0.006
0.2310	4.074±0.004	3.655±0.005	4.794±0.006	39.32±0.036	608.4±0.006
0.3185	4.015±0.004	3.589±0.005	4.701±0.006	38.97±0.034	617.4±0.006
0.4448	3.993±0.004	3.565±0.005	4.667±0.006	38.83±0.033	620.8±0.006
0.5516	3.978±0.004	3.548±0.005	4.644±0.006	38.74±0.033	623.1±0.006
0.6431	3.968±0.004	3.536±0.005	4.628±0.006	38.68±0.032	624.7±0.006
0.8278	3.951±0.004	3.517±0.005	4.601±0.006	38.57±0.032	627.4±0.006
1	3.938±0.004	3.503±0.005	4.581±0.006	38.49±0.031	629.4±0.006
$T = 308.15 \text{ K}$					
0	4.607±0.004	4.336±0.006	5.647±0.008	43.61±0.059	556.1±0.006
0.0477	4.426±0.004	4.119±0.006	5.352±0.008	42.50±0.051	578.9±0.006
0.0790	4.387±0.004	4.072±0.006	5.290±0.007	42.26±0.049	584.0±0.006
0.1178	4.307±0.004	3.977±0.006	5.163±0.007	41.76±0.046	594.8±0.006
0.1668	4.235±0.004	3.890±0.005	5.048±0.007	41.31±0.043	604.9±0.006
0.2310	4.174±0.004	3.821±0.005	4.951±0.007	40.94±0.041	613.7±0.006
0.3185	4.126±0.004	3.767±0.005	4.876±0.007	40.65±0.039	620.9±0.006
0.4448	4.110±0.004	3.749±0.005	4.850±0.007	40.55±0.039	623.4±0.006
0.5516	4.094±0.004	3.731±0.005	4.756±0.007	40.45±0.038	632.6±0.006
0.6431	4.083±0.004	3.718±0.005	4.807±0.007	40.38±0.038	627.5±0.006
0.8278	4.064±0.004	3.696±0.005	4.777±0.006	40.27±0.037	630.4±0.006
1	4.050±0.004	3.681±0.005	4.756±0.006	40.18±0.037	632.6±0.006

Table IV. Coefficients of Redlich–Kister (R–K) equation and standard deviation ( $\sigma$ ) values for liquid PEG-400 + DMSO at different temperatures

$T / \text{K}$	Parameter	$A_0$	$A_1$	$A_2$	$A_3$	$A_4$	$\sigma$
288.15	$K_s^E$	-9.237	5.450	-7.918	13.088		0.271
		-9.922	7.449	-9.754	11.338		0.126
		-10.794	10.231	-10.702	6.867		0.130
288.15	$K_T^E$	-12.872	7.619	-11.114	18.283		0.372
		-13.665	10.123	-13.263	15.734		0.183
		-14.665	13.650	-14.187	9.448		0.182
288.15	$L_f^E$	-4.883	2.911	-4.021	6.573		0.141
		-5.201	3.947	-4.950	5.565		0.064
		-5.614	5.390	-5.399	3.116		0.066
288.15	$P_i^E$	12.517	-11.399	-10.435	0.046	38.408	0.474
		12.300	-11.202	0.828	-3.901	18.772	0.082
		12.326	-12.213	9.205	-3.403	2.610	0.160
288.15	$V_f^E$	-0.818	0.487	-0.692	1.131		0.004
		-0.859	0.640	-0.820	0.957		0.001
		-0.913	0.856	-0.869	0.550		0.001

The inspection of Fig. 2 reveals that the  $K_s^E$  is throughout negative in the given concentration range at 288.15 K. The overall negative trend of  $K_s^E$  indi-

cates the presence of a hydrogen bonding between PEG-400 and DMSO.<sup>54</sup> Moreover, a close look at Fig. 2 shows that the magnitude of negative deviation is the highest around  $X_1 \approx 0.3$ . Furthermore, Fig. 2 displays that at temperatures 298.15 and 308.15 K, a similar behaviour is observed for the PEG-400 and DMSO binary system. However, a slight increase in the negative value of  $K_s^E$  is obvious. This is expected because a rise in temperature enhances the kinetic energy of molecules, leading to the weakening of molecular interactions. The variations in  $K_T^E$  values with changes in mole fraction ( $X_1$ ) and rise in temperature (Fig. 3) are similar to the variations observed for  $K_s^E$  values with such changes.

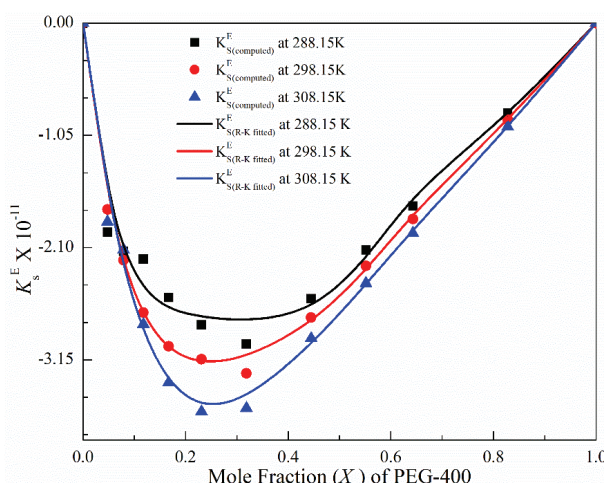


Fig. 2. Excess adiabatic compressibility ( $K_s^E$ ) for PEG-400 + DMSO at different temperatures. The solid curves represent the Redlich–Kister equation fitting.

Since the intermolecular free length ( $L_f$ ) and adiabatic compressibility ( $K_s$ ) are directly related to each other, so with the increase in  $K_s$  values, an increase in  $L_f$  values is expected.<sup>55</sup> Table III reports that both  $K_s$  and  $L_f$  are decreasing with the rise in the mole fraction ( $X_1$ ) of PEG-400. It is likely due to the quick uncoiling of the small-sized chain (carbon atoms = 17) of PEG-400 in a highly polar aprotic organo-sulphur solvent DMSO (dipole moment = 3.96 D\*), due to the dipole-induced dipole and hydrogen bonding interactions between solute and solvent molecules. The rise in the temperature from 298.15 to 308.15 K for the mixture shows a slight increase in  $K_s$  and  $L_f$  values, which is expected, as the enhancement of thermal agitations in the system leads to a higher mobility of the molecules. The excess intermolecular free length ( $L_f^E$ ) is directly linked to the weakening of intra-molecular interactions and the formation of H-bonding in the sys-

\* 1 D =  $3.335 \times 10^{-30}$  C m

tem.<sup>54,55</sup> The overall negative value of  $L_f^E$  for the mixture (Fig. 4) points to the presence of inter-molecular H-bonding in the system. The minimum value of  $L_f^E$  occurs around  $X_1 \approx 0.3$ , indicating the presence of the greatest strength of hydrogen bonding at that concentration. The order of strength of intermolecular interactions with the increase in temperature is  $(L_f^E)_{288.15\text{ K}} > (L_f^E)_{298.15\text{ K}} > (L_f^E)_{308.15\text{ K}}$ .

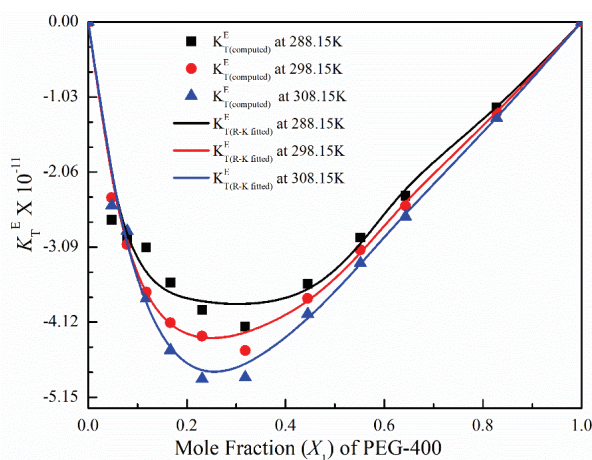


Fig. 3. Excess isothermal compressibility ( $K_T^E$ ) for PEG-400 + DMSO at different temperatures. The solid curves represent the Redlich–Kister equation fitting.

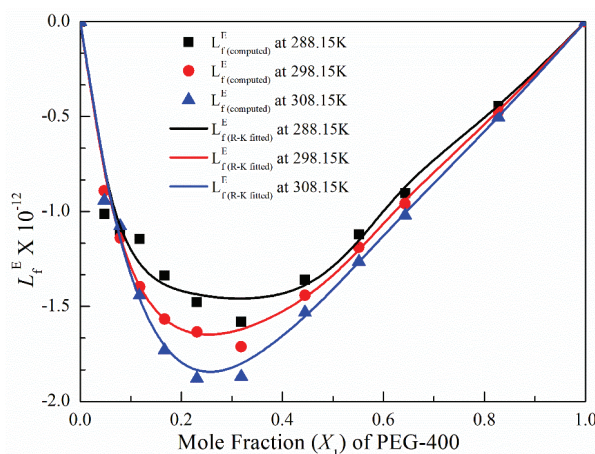


Fig. 4. Excess free length ( $L_f^E$ ) for PEG-400 + DMSO at different temperatures. The solid curves represent the Redlich–Kister equation fitting.

The internal pressure ( $P_i$ ), the result of the molecules' attractive and repulsive interactions, is a parameter that is sensitive to all three types of interactions, *viz.*, solute–solute (A–A), solute–solvent (A–B), and solvent–solvent (B–B) inter-

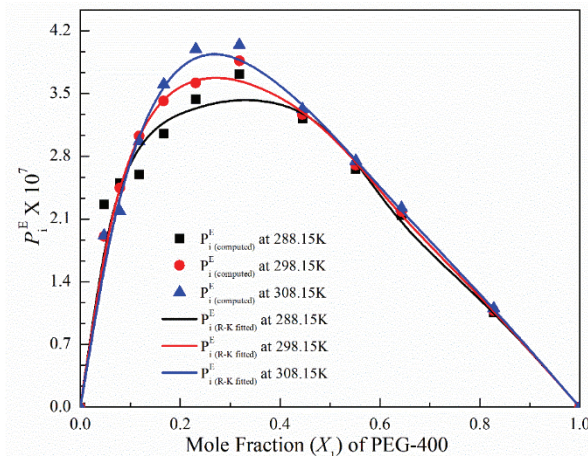


Fig. 5. Excess internal pressure ( $P_i^E$ ) for PEG-400 + DMSO at different temperatures. The solid curves represent the Redlich–Kister equation fitting.

actions, in a mixture.<sup>56</sup> The excess internal pressure ( $P_i^E$ ) is also very sensitive to the variations in the strength of the intermolecular interactions. Fig. 5 exhibits that  $P_i^E$  is positive over the entire mole fraction ( $X_1$ ) range. It confirms that the A–B interactions dominate over A–A and B–B interactions. Rao *et al.*,<sup>57</sup> reported that an increase in  $P_i$  values leads to a decrease in free volume ( $V_f^E$ ). The negative values of  $V_f^E$  throughout the concentration range (Fig. 6) point to the enhancement

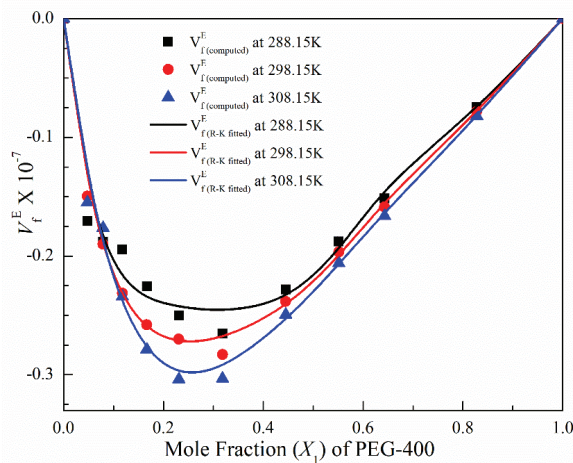


Fig. 6. Excess free volume ( $V_f^E$ ) for PEG-400 + DMSO at different temperatures. The solid curves represent the Redlich–Kister equation fitting.

of compactness among the molecules of the mixture, confirming the existence of attractive interactions in the system.<sup>58</sup> Excess parameters, *viz.*,  $V_f^E$ ,  $K_s^E$ ,  $K_T^E$ ,  $L_f^E$

and  $P_i^E$  for the binary mixture studied here, are fitted with the R-K polynomial equation, determined by the least-square regression method. Table IV reports the R-K polynomial coefficients for the system in the temperature range of 288.15 to 308.15 K. The low  $\sigma$  values points to the suitability of the R-K polynomial equation for the system under study at all the temperatures investigated here.

#### *Partial and apparent molar volumes*

For the given system of PEG-400 + DMSO, the partial molar volume ( $\bar{V}_1, \bar{V}_2$ ), excess partial molar volume ( $\bar{V}_1^E, \bar{V}_2^E$ ), apparent molar volume ( $V_{\varphi_1}, V_{\varphi_2}$ ) and apparent molar volume at infinite dilution ( $\bar{V}_{\varphi_1}^\infty, \bar{V}_{\varphi_2}^\infty$ ) is calculated and presented in Tables V and VI. Partial molar volumes and apparent molar volumes of solute and solvent are obtained using the standard procedure reported below (Eqs. (16)–(19)).<sup>59,60</sup>

$$\bar{V}_1 = V + (1 - X_1) \frac{\partial V}{\partial X_1} \quad (16)$$

$$\bar{V}_2 = V + (1 - X_2) \frac{\partial V}{\partial X_2} \quad (17)$$

$$V_{\varphi_1} = V_1 + \frac{V_m^E}{X_1} \quad (18)$$

$$V_{\varphi_2} = V_2 + \frac{V_m^E}{X_2} \quad (19)$$

Here,  $V_m^E$  is the molar excess volume.

TABLE V. Partial volume, excess partial molar volume and apparent molar volume for PEG-400(1) + DMSO (2) at different temperatures; the standard uncertainties ( $u$ ) are  $u(T) = 0.01$  K,  $u(d) = 0.5$  kg m<sup>-3</sup>,  $u(U) = 1.0$  m s<sup>-1</sup> and  $U(x_1) = 0.0001$  kg/mol

$X_1$	$V_1$	$V_2$	$V_1^E$	$V_2^E$	$V_{\varphi_1}$	$V_{\varphi_2}$
	cm <sup>3</sup> mol <sup>-1</sup>					
288.15 K						
0	348.87±0.158	70.66±0.032	-5.015	0.000	—	70.66±0.032
0.0477	349.79±0.157	70.61±0.032	-4.096	-0.046	348.87±0.157	70.41±0.032
0.0790	352.60±0.158	70.40±0.032	-1.290	-0.254	349.64±0.156	70.29±0.031
0.1178	354.62±0.158	70.22±0.031	0.738	-0.435	351.37±0.157	70.32±0.031
0.1668	352.46±0.157	70.67±0.032	-1.428	0.008	352.50±0.157	70.38±0.031
0.2310	351.97±0.156	70.58±0.031	-1.919	-0.075	351.72±0.156	70.01±0.031
0.3185	353.66±0.157	70.10±0.031	-0.230	-0.561	352.45±0.156	69.99±0.031
0.4448	353.75±0.157	69.98±0.031	-0.135	-0.680	352.90±0.156	69.87±0.031
0.5516	353.96±0.157	69.82±0.031	0.071	-0.838	353.28±0.157	69.91±0.031
0.6431	353.92±0.157	69.87±0.031	0.037	-0.786	353.49±0.157	69.94±0.031
0.8278	353.90±0.157	69.95±0.031	0.010	-0.708	353.75±0.157	70.00±0.031
1	353.89±0.157	70.00±0.031	0.000	-0.661	353.89±0.157	—

TABLE V. Continued

$X_1$	$V_1$ $\text{cm}^3 \text{ mol}^{-1}$	$V_2$ $\text{cm}^3 \text{ mol}^{-1}$	$\bar{V}_1^E$ $\text{cm}^3 \text{ mol}^{-1}$	$\bar{V}_2^E$ $\text{cm}^3 \text{ mol}^{-1}$	$V_{\varphi_1}$ $\text{cm}^3 \text{ mol}^{-1}$	$V_{\varphi_2}$ $\text{cm}^3 \text{ mol}^{-1}$
298.15 K						
0	351.51±0.160	71.30±0.033	-5.000	0.000	-	71.30±0.033
0.0477	354.38±0.160	71.16±0.032	-2.130	-0.144	351.51±0.159	71.05±0.032
0.0790	357.41±0.162	71.00±0.032	0.901	-0.301	353.90±0.160	71.08±0.032
0.1178	357.86±0.162	70.95±0.032	1.345	-0.353	355.21±0.160	71.13±0.032
0.1668	356.53±0.161	71.24±0.032	0.022	-0.069	356.19±0.161	71.24±0.032
0.2310	354.47±0.159	71.69±0.032	-2.042	0.390	355.77±0.160	71.08±0.032
0.3185	355.28±0.159	71.24±0.032	-1.229	-0.066	355.14±0.159	70.66±0.032
0.4448	356.59±0.159	70.61±0.032	0.082	-0.692	355.73±0.159	70.68±0.032
0.5516	356.61±0.159	70.61±0.032	0.099	-0.696	356.04±0.159	70.73±0.032
0.6431	356.56±0.159	70.68±0.032	0.051	-0.624	356.22±0.159	70.77±0.032
0.8278	356.52±0.159	70.79±0.032	0.014	-0.515	356.42±0.159	70.86±0.032
1	356.51±0.159	70.86±0.032	0.000	-0.449	356.51±0.159	-
308.15 K						
0	355.86±0.164	71.86±0.033	-3.292	0.000	-	71.86±0.033
0.0477	359.39±0.164	71.69±0.033	0.236	-0.177	355.86±0.163	71.70±0.033
0.0790	361.29±0.165	71.65±0.033	2.137	-0.214	358.80±0.164	71.83±0.033
0.1178	360.56±0.164	71.67±0.033	1.405	-0.193	359.11±0.164	71.86±0.033
0.1668	359.06±0.163	72.03±0.033	-0.094	0.166	359.89±0.164	72.01±0.033
0.2310	356.96±0.162	72.42±0.033	-2.195	0.558	358.82±0.163	71.76±0.033
0.3185	358.03±0.162	71.97±0.032	-1.119	0.104	358.26±0.162	71.44±0.032
0.4448	359.05±0.162	71.41±0.032	-0.098	-0.452	358.49±0.161	71.33±0.032
0.5516	359.26±0.162	71.25±0.032	0.112	-0.609	358.77±0.161	71.39±0.032
0.6431	359.21±0.162	71.34±0.032	0.058	-0.527	358.92±0.161	71.44±0.032
0.8278	359.17±0.162	71.46±0.032	0.015	-0.404	359.08±0.161	71.53±0.032
1	359.15±0.162	71.53±0.032	0.000	-0.330	359.15±0.161	-

TABLE VI. Molar volume and apparent molar volume at infinite dilution for PEG-400(1) + DMSO (2) at different temperatures

$T / \text{K}$	$V_1$ $\text{cm}^3 \text{ mol}^{-1}$	$V_2$ $\text{cm}^3 \text{ mol}^{-1}$	$\bar{V}_{\varphi_1}^{\infty}$ $\text{cm}^3 \text{ mol}^{-1}$	$\bar{V}_{\varphi_2}^{\infty}$ $\text{cm}^3 \text{ mol}^{-1}$
288.15	353.89	70.66	350.44	70.40
298.15	356.51	71.30	354.11	71.16
308.15	359.15	71.86	358.22	71.85

The values of  $\bar{V}_{\varphi_1}^{\infty}$  and  $\bar{V}_{\varphi_2}^{\infty}$  are determined using the analytical extrapolation methods. In this approach,  $\bar{V}_{\varphi_1}^{\infty}$  is obtained by taking  $V_{\varphi_1}$  to  $X_1 = 0$  ( $X_2 = 1$ ) and  $\bar{V}_{\varphi_2}^{\infty}$  is obtained by taking the  $V_{\varphi_2}$  to  $X_2 = 0$  ( $X_1 = 1$ ).

The portray of Table V indicate that in general, the excess partial volumes are negative at all temperatures. It is well mentioned in literature that, the negative values of  $\bar{V}_1^E$  and  $\bar{V}_2^E$  is an indicative of intermolecular interaction by hydrogen bonding or due to the geometrical fitting of one component into another.<sup>61</sup> These findings are in agreement with the results arrived earlier for the given sys-

tem PEG-400 + DMSO. The apparent molar volume at infinite dilution is an important property to access the solute-solvent interaction of the liquid mixtures. At infinite dilution, the apparent molar volume only depends upon the solute–solvent interaction, and the contribution of solute–solute interactions disappears in the mixture; furthermore, at infinite dilution, solute–solvent interaction becomes independent of the composition of the mixture.<sup>61</sup> The apparent molar volume for a solute and a solvent at different temperatures are reported in Table VI. The inspection of Table VI reveals that the apparent molar volume at infinite dilution for PEG-400 and DMSO is less than that of pure molar volume, which confirms that the solute–solvent interactions in the system are present.<sup>60</sup> Furthermore, the differences  $\bar{V}_{\phi_1}^{\infty} - V_1$  and  $\bar{V}_{\phi_2}^{\infty} - V_2$  decrease with temperature, which indicates that the solute–solvent interactions get weaker with the rise in temperature.

#### *Theoretical estimation of ultrasonic velocity of the mixture*

Using various standard relations such as the ideal mixing relation (IMR), Nomoto relation (NR), impedance dependence relation (IDR), van Deal–Vangeel relation (VVR), Junjie relation (JR), Schaaff's collision factor theory (CFT) and the ultrasonic velocities in the PEG-400 + DMSO mixture have been determined. The experimentally measured values of ultrasonic velocity ( $U^*$ ) along with theoretically predicted  $U_{\text{IM}}$ ,  $U_{\text{N}}$ ,  $U_{\text{Z}}$ ,  $U_{\text{V}}$ ,  $U_{\text{J}}$ , and  $U_{\text{CFT}}$  values at 288.15, 298.15 and 308.15 K, for the binary mixture under study are reported in Table VII. It is ob-

TABLE VII. Experimental ( $U^*$ ) and calculated ultrasonic velocity using different mixing rules for PEG-400 + DMSO at different temperatures

$X_1$	$U^*$	$U_{\text{IM}}$	$U_{\text{N}}$	$U_{\text{Z}}$	$U_{\text{V}}$	$U_{\text{J}}$	$U_{\text{CFT}}$
T = 288.15 K							
0	1524	1524	1524	1524	1524	1524	1513
0.0477	1564	1529	1545	1529	1422	1543	1529
0.0790	1569	1533	1555	1533	1370	1553	1536
0.1178	1574	1537	1566	1537	1317	1563	1541
0.1668	1587	1542	1576	1542	1264	1574	1545
0.2310	1598	1549	1587	1549	1213	1584	1553
0.3185	1613	1558	1597	1558	1169	1595	1557
0.4448	1618	1571	1608	1572	1140	1606	1560
0.5516	1621	1582	1614	1583	1144	1613	1561
0.6431	1623	1592	1619	1592	1168	1618	1561
0.8278	1627	1611	1625	1612	1296	1625	1561
1	1629	1629	1629	1629	1629	1629	1560
T = 298.15 K							
0	1490	1490	1490	1490	1490	1490	1510
0.0477	1523	1495	1511	1495	1390	1509	1527
0.0790	1534	1498	1521	1499	1339	1519	1532
0.1178	1548	1502	1532	1503	1287	1529	1536

TABLE VII. Continued

$X_1$	$U^*$	$U_{IM}$	$U_N$	$U_Z$	$U_V$	$U_J$	$U_{CFT}$
T = 298.15 K							
0.1668	1559	1508	1542	1508	1236	1539	1541
0.2310	1568	1514	1553	1515	1186	1550	1547
0.3185	1579	1524	1563	1524	1143	1561	1554
0.4448	1584	1537	1574	1537	1115	1572	1557
0.5516	1587	1548	1580	1549	1119	1579	1558
0.6431	1589	1558	1584	1558	1142	1583	1559
0.8278	1592	1577	1591	1577	1268	1590	1559
1	1595	1595	1595	1595	1595	1595	1558
T = 308.15 K							
0	1457	1457	1457	1457	1457	1457	1507
0.0477	1489	1462	1477	1462	1359	1475	1523
0.0790	1497	1465	1488	1465	1309	1485	1526
0.1178	1513	1469	1498	1469	1258	1495	1532
0.1668	1529	1474	1509	1474	1208	1506	1536
0.2310	1540	1481	1519	1481	1160	1516	1544
0.3185	1548	1490	1530	1491	1117	1527	1551
0.4448	1550	1503	1540	1504	1090	1539	1555
0.5516	1553	1515	1547	1515	1094	1545	1556
0.6431	1555	1524	1551	1525	1117	1550	1557
0.8278	1559	1544	1558	1544	1240	1557	1557
1	1562	1562	1562	1562	1562	1562	1557

TABLE VIII. Absolute percentage deviation ( $APD$ ) for ultrasonic velocity mixing rules applied on PEG-400 + DMSO at different temperatures

T / K	$U_{IM}$	$U_N$	$U_Z$	$U_V$	$U_J$	$U_{CFT}$
288.15	2.0	0.5	2.0	18.1	0.6	3.0
298.15	2.1	0.6	2.1	18.2	0.7	1.1
308.15	2.2	0.6	2.2	18.3	0.8	-0.8

erved that  $U_N$  and  $U_J$  are well matches with  $U^*$ , whereas  $U_{IM}$ ,  $U_Z$  and  $U_{CFT}$  are showing a reasonable agreement with the experimental values. However,  $U_V$  values show a large departure from experimental values. Thereby, the VVR fails to determine the ultrasonic velocity values in the given temperature and concentration range for the system. It is likely due to the large difference in size of the molecules of PEG-400 and DMSO. To have a better understanding of the compatibility of these relations to predict the ultrasonic velocity in the given concentration and temperature range for the system, the absolute percentage deviation ( $APD$ ) values were determined. These values are presented in Table VIII. It is worth noting here that  $APD$  values for  $U_N$  (NR) and  $U_J$  (JR) are  $<1\%$ ,  $\sim 2\%$  for  $U_{IM}$  (IMR) and  $U_Z$  (IDR), respectively, and  $\sim 18\%$  for  $U_V$  (VVR) at all the working temperatures. Moreover, the  $APD$  value for CFT is  $<1\%$  at 308.15 K, 3.0 % at 288.15 K and 1.1 % at 298.15 K. Thus, it can be concluded that except

VVR, the other five relations investigated here can be successfully employed to predict the ultrasonic velocity for the system, in the given concentration range and at all working temperatures.

#### *UV-Vis spectra*

The UV-Vis spectra of PEG-400 with DMSO is presented in Fig. 7. A close look at Fig. 7 reveals that the absorption peak of PEG-400 is shifted from 247 to 253 nm, as DMSO concentration increases in the mixture, which indicates the possibility of hydrogen bonding between the hydrogen of the hydroxyl group of PEG-400 and the free lone pair of oxygen atom of DMSO, *i.e.*,  $(\text{CH}_3)_2\text{S}=\text{O}-\text{H}-(\text{OCH}_2-\text{CH}_2-\text{O})\text{PEG}-\text{H}-\text{O}=\text{S}(\text{CH}_3)_2$ .<sup>35</sup> It can be attributed to the  $\text{n}\rightarrow\pi^*$  electronic transition of the unshaped electronic pair of oxygen atoms in DMSO.

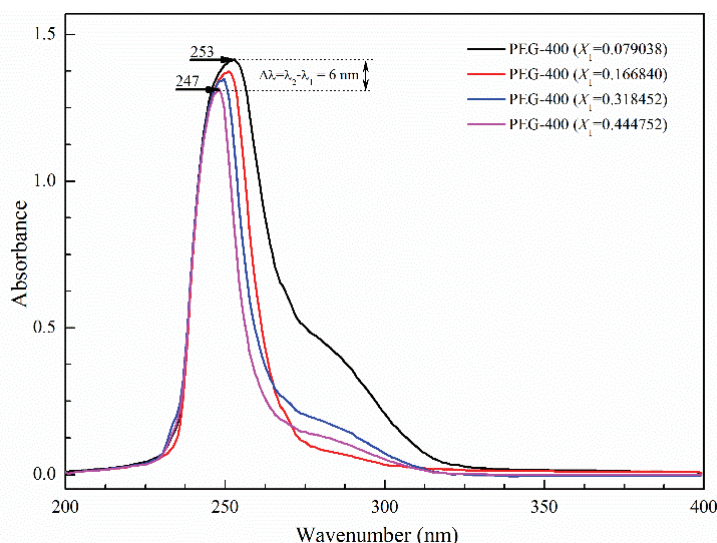


Fig. 7. UV-Vis spectra of PEG-400 + DMSO at increasing concentrations of DMSO.

#### *FTIR spectra*

The FTIR spectra of pure DMSO, pure PEG-400 and their binary mixture are presented in Fig. 8a–e, respectively. The perusal of spectra of pure DMSO (Fig. 8a) indicates a peak at wave number  $3430.65\text{ cm}^{-1}$ , which is indicative of O–H stretching.

A peak at  $1019.25\text{ cm}^{-1}$  describes the C–S stretching vibrations of molecules. The close look to Fig. 8 also infers a considerable shift ( $36\text{--}48\text{ cm}^{-1}$ ) as well as a broadening in the  $3445.39\text{ cm}^{-1}$  peak with the change in concentration DMSO in the mixtures (Fig 8c–e), which is most likely due to the breaking of the intra-molecular interactions of PEG-400 and the formation of intermolecular

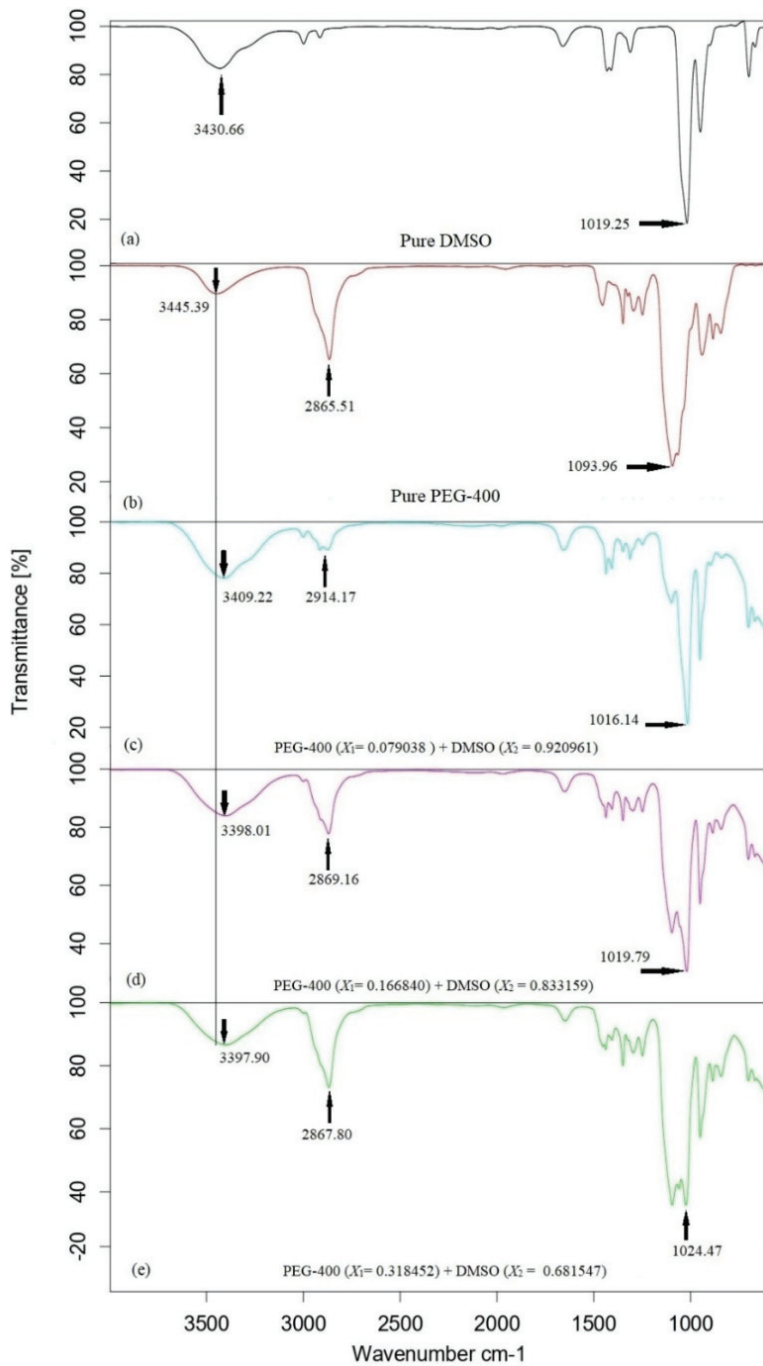


Fig. 8. FTIR spectra of pure PEG-400, pure DMSO and PEG-400 + DMSO at different concentrations.

H-bonding between PEG-400 and DMSO molecules. Moreover, when the amount of PEG-400 (solute) is increased in the mixture the peak, at wave number  $1019.25\text{ cm}^{-1}$  of pure DMSO (Fig. 8a), splits into two peaks. It indicates the presence of intermolecular interactions and the formation of a dimer in the system.<sup>19</sup> The conclusions based on FTIR spectra of the binary mixtures supplement the findings obtained using the ultrasonic technique for the system.

#### CONCLUSION

New experimental values of ultrasonic velocity and density have been determined for a polymer mixture of PEG-400 and DMSO at 288.15, 298.15 and 308 K. The validity of various mixing rules for the ultrasonic velocity has also been tested for the given mixtures. Based on the ultrasonic velocity and the density, some important physical parameters and their excess values are also computed. The current investigation confirms the intermolecular H-bonding between PEG-400 and DMSO molecules. The spectroscopic analysis of the given system also confirms the presence of intermolecular H-bonding between PEG-400 and DMSO. Additionally different temperatures. It can be concluded that out of six mixing rules, the Nomoto relation and the Junjie relation are found to be best suited for the given mixture. Overall, this insightful analysis of the given mixtures can find the use in industry for solvent selection, design, extraction and separation processes.

#### SUPPLEMENTARY MATERIAL

Additional data and information are available electronically at the pages of journal website: <https://www.shd-pub.org.rs/index.php/JSCS/article/view/12720>, or from the corresponding author on request.

#### ИЗВОД

#### ИСПИТИВАЊЕ МОЛЕКУЛАРНИХ ИНТЕРАКЦИЈА БИНАРНИХ МЕШАВИНА PEG-400 И DMSO НА РАЗЛИЧИТИМ ТЕМПЕРАТУРАМА УЛТРАЗВУКОМ И СПЕКТРОСКОПСКОПИЈОМ ИСТРАГЕ

MONIKA DHIMAN<sup>1</sup>, ARUN UPMANYU<sup>1\*</sup>, DEVINDER PAL SINGH<sup>2</sup> и KAILASH CHANDRA JUGLAN<sup>3</sup>

<sup>1</sup>Chitkara University Institute of Engineering and Technology, Chitkara University, Punjab, 140401, India,  
<sup>2</sup>Acoustics Research Center, Mississauga, L5A 1Y7, Ontario, Canada и <sup>3</sup>Department of Physics, Lovely Faculty of Technology and Sciences, Lovely Professional University, Punjab, India

У раду су приказани резултати мерења ултразвучне брзине и густине бинарне смеше поли(етилен-гликола), PEG-400 и диметил-сулфоксида (DMSO), при различитим концентрацијама и различитим температурама (288,15, 298,15 и 308,15 K), који су додатно искоришћени за утврђивање неколико физичких параметара као што су адиабатска и изотермална компресија, интермолекуларна слободна дужина, унутрашњи притисак и слободна запремина. Вишак вредности ових параметара је такође израчунат и фитована са Redlich-Kister (R-K) полиномном једначином. Природа, тип и јачина интермолекуларних интеракција присутних у PEG-400 + DMSO смеши објашњени су помоћу основе знака и величине вишке вредности. Поред тога одређени су парцијална запремина,

вишак парцијалне запремине и моларна запремина при бесконачном разблаживању да би се испитале интеракције растворак–растварач. Разна правила мешања као што су идеално правило мешања ( $U_{im}$ ), Nomoto ( $U_N$ ), однос зависности од импедансе ( $U_z$ ), Junjie ( $U_J$ ), van Deal–Vangeel ( $U_V$ ) и теорија фактора судара ( $U_{CFT}$ ) су употребљена за израчунавање ултразвучне брзине и упоређени са експерименталним резултатима. Nomoto и Junjie једначине најбоље описују испитивану смешу. Систем је такође испитан коришћењем FTIR и UV–Vis спектроскопском. Промена интензитета и померање пика у FTIR и UV–Vis спектрима PEG-400 + DMSO смеше су потврдиле водоничне везе у систему.

(Примљено 7. децембра 2023, ревидирано 22. јануара, прихваћено 2. јуна 2024)

#### REFERENCES

1. P. Malik, G. Chauhan, P. Kumar, A. Deep, *Liq. Cryst.* **49** (2022) 2008 (<https://doi.org/10.1080/02678292.2022.2094006>)
2. P. Kumar, V. Sharma, P. Malik, K. K. Raina, *J. Mol. Struct.* **1196** (2019) 866 (<https://doi.org/10.1016/j.molstruc.2019.06.045>)
3. S. Tian, Y. Hou, W. Wu, S. Ren, J. Qian, *J. Hazard. Mater.* **278** (2014) 409 (<https://doi.org/10.1016/j.jhazmat.2014.06.037>)
4. K. T. Lee, A. R. Mohamed, S. Bhatia, K. H. Chu, *J. Chem. Eng.* **114** (2005) 171 (<https://doi.org/10.1016/j.cej.2005.08.020>)
5. T. Zhao, J. Zhang, B. Guo, F. Zhang, F. Sha, X. Xie, X. Wei, *J. Mol. Liq.* **207** (2015) 315 (<https://doi.org/10.1016/j.molliq.2015.04.001>)
6. K. Zhang, J. Yang, X. Yu, J. Zhang, X. Wei, *J. Chem. Eng. Data* **56** (2011) 3083 (<https://doi.org/10.1021/je200148u>)
7. J. Rodríguez-Sevilla, M. Álvarez, G. Limiñana, M. C. Díaz, *J. Chem. Eng. Data* **47** (2002) 1339 (<https://doi.org/10.1021/je015538e>)
8. D. Nagel, R. de Kermadec, H. G. Lintz, C. Roizard, F. Lapicque, *Chem. Eng. Sci.* **57** (2002) 4883 ([https://doi.org/10.1016/S0009-2509\(02\)00283-X](https://doi.org/10.1016/S0009-2509(02)00283-X))
9. F. Han, J. Zhang, G. Chen, X. Wei, *J. Chem. Eng. Data* **53** (2008) 2598 (<https://doi.org/10.1021/je800464t>)
10. S. Trivedi, C. Bhanot, S. Pandey, *J. Chem. Thermodyn.* **42** (2010) 1367 (<https://doi.org/10.1016/j.jct.2010.06.001>)
11. A. Upmanyu, M. Dhiman, D. P. Singh, H. Kumar, *J. Mol. Liq.* **334** (2021) 115939 (<https://doi.org/10.1016/j.molliq.2021.115939>)
12. B. V. Kumar Naidu, K. C. Rao, M. C. S. Subha, *J. Chem. Eng. Data* **47** (2002) 379 (<https://doi.org/10.1021/je0101395>)
13. M. Dhiman, K. Singh, J. Kaushal, A. Upmanyu, D. P. Singh, *Acta Acust. United Acust.* **105** (2019) 743 (<https://doi.org/10.3813/AAA.919354>)
14. M. Rani, S. Gahlyan, A. Gaur, S. Maken, *Chin. J. Chem. Eng.* **23** (2015) 689 (<https://doi.org/10.1016/j.cjche.2014.12.003>)
15. P. Kaur, N. Chakraborty, K. C. Juglan, H. Kumar, *J. Mol. Liq.* **315** (2020) 113763 (<https://doi.org/10.1016/j.molliq.2020.113763>)
16. D. P. Gupta, A. Upmanyu, M. Dhiman, D. P. Singh, Estimation of ultrasonic velocity and viscosity of polymer solutions of HTPB+ chlorobenzene at different temperatures, AIP Conf. Proc., AIP Publishing, Melville, NY, 2022 (<https://doi.org/10.1063/5.0080974>)
17. A. Ali, A. K. Nain, V. K. Sharma, S. Ahmad, *Phys. Chem. Liq.* **42** (2004) 375 (<https://doi.org/10.1080/00319100410001679882>)

18. M. Umadevi, R. Kesavasamy, K. Rathina, R. Mahalakshmi, *J. Mol. Liq.* **219** (2016) 820 (<https://doi.org/10.1016/j.molliq.2016.03.085>)
19. L. Ma, F. Sha, X. Qiao, Q. Li, J. Zhang, *Chin. J. Chem. Eng.* **25** (2017) 1249 (<https://doi.org/10.1016/j.cjche.2017.01.001>)
20. G. Arivazhagan, A. Elangovan, R. Shanmugam, R. Vijayalakshmi, N. K. Karthick, *J. Mol. Liq.* **214** (2016) 357 (<https://doi.org/10.1016/j.molliq.2015.10.062>)
21. L. M. Madikizela, P. S. Mdluli, L. Chimuka, *React. Funct. Polym.* **103** (2016) 33 (<https://doi.org/10.1016/j.reactfunctpolym.2016.03.017>)
22. T. S. Krishna, K. Raju, M. Gowrisankar, A. K. Nain, B. Munibhadrayya, *J. Mol. Liq.* **216** (2016) 484 (<https://doi.org/10.1016/j.molliq.2016.01.085>)
23. A. Awasthi, J. P. Shukla, *Ultrasonics* **41** (2003) 477 ([https://doi.org/10.1016/S0041-624X\(03\)00127-6](https://doi.org/10.1016/S0041-624X(03)00127-6))
24. P. Malik, S. Kumar, Khushboo, A. Upmanyu, P. Kumar, P. Malik, *Liq. Cryst.* **49** (2022) 1604 (<https://doi.org/10.1080/02678292.2022.2102684>)
25. O. E.-A. A. Adam, A. A. Hassan, *Phys. Chem. Liq.* **56** (2018) 55 (<https://doi.org/10.1080/00319104.2017.1292424>)
26. N. Chaudhary, A. Kumar Nain, *Phys. Chem. Liq.* **58** (2020) 736 (<https://doi.org/10.1080/00319104.2019.1636378>)
27. M. T. Zafarani-Moattar, N. Tohidifar, *J. Chem. Eng. Data* **51** (2006) 1769 (<https://doi.org/10.1021/je0601715>)
28. M. T. Zafarani-Moattar, N. Tohidifar, *J. Chem. Eng. Data* **53** (2008) 785 (<https://doi.org/10.1021/je700651e>)
29. H. Patel, Z. S. Vaid, U. U. More, S. P. Ijardar, N. I. Malek, *J. Chem. Thermodyn.* **99** (2016) 40 (<https://doi.org/10.1016/j.jct.2016.02.025>)
30. F. M. Sannaningannavar, B. S. Navati, N. H. Ayachit, *J. Therm. Anal. Calorim.* **112** (2013) 1573 (<https://doi.org/10.1007/s10973-012-2724-5>)
31. J. G. Baragi, M. I. Aralaguppi, T. M. Aminabhavi, M. Y. Kariduraganavar, A. S. Kittur, *J. Chem. Eng. Data* **50** (2005) 910 (<https://doi.org/10.1021/je049610v>)
32. S. Baluja, R. M. Talaviya, *J. Chem. Eng. Data* **61** (2016) 1431 (<https://doi.org/10.1021/acs.jced.5b00627>)
33. V. K. Syal, S. Chauhan, R. Gautam, *Ultrason.* **36** (1998) 619 ([https://doi.org/10.1016/S0041-624X\(97\)00104-2](https://doi.org/10.1016/S0041-624X(97)00104-2))
34. D. Keshapolla, R. L. Gardas, *Fluid Phase Equilib.* **383** (2014) 32 (<https://doi.org/10.1016/j.fluid.2014.09.022>)
35. T. Zhao, Q. Xu, J. Xiao, X. Wei, *J. Chem. Eng. Data* **60** (2015) 2135 (<https://doi.org/10.1021/acs.jced.5b00209>)
36. A. Ali, F. Nabi, *J. Dispers. Sci. Technol.* **31** (2010) 1326 (<https://doi.org/10.1080/01932690903227469>)
37. H. Wang, W. Liu, J. Huang, *J. Chem. Thermodyn.* **36** (2004) 743 (<https://doi.org/10.1016/j.jct.2004.04.004>)
38. R. K. Shukla, S. N. Dixit, P. Jain, P. Mishra, S. Sharma, *Orbital-Electron. J. Chem.* **2** (2011) 356 (<https://periodicos.ufms.br/index.php/orbital/article/view/17980/12479>)
39. J. C. De La Torre, *Ann. N. Y. Acad. Sci.* **411** (1983) 293 (<https://doi.org/10.1111/j.1749-6632.1983.tb47311.x>)
40. M. T. Zafarani-Moattar, H. Shekaari, *J. Chem. Thermodyn.* **38** (2006) 624 (<https://doi.org/10.1016/j.jct.2005.07.018>)
41. A. Ali, A. K. Nain, D. Chand, R. Ahmad, *Bull. Chem. Soc. Jpn.* **79** (2006) 702 (<https://doi.org/10.1246/bcsj.79.702>)

42. J. Krakowiak, D. Bobicz, W. Grzybkowski, *J. Mol. Liq.* **88** (2000) 197 ([https://doi.org/10.1016/S0167-7322\(00\)00154-9](https://doi.org/10.1016/S0167-7322(00)00154-9))
43. H. Shekaari, M. T. Zafarani-Moattar, *Int. J. Thermophys.* **29** (2008) 534 (<https://doi.org/10.1007/s10765-008-0395-z>)
44. S. R. Dandwate, S. B. Deshmukh, *J. Curr. Pharma Res.* **10** (2020) 3716 (ISSN-2230-7842 CODEN-CPRUE6, [www.jcpronline.in/](http://www.jcpronline.in/))
45. U. R. Kapadi, S. K. Chavan, O. S. Yemul, *J. Chem. Eng. Data* **42** (1997) 548 ([https://doi.org/10.1021/je960216+\)](https://doi.org/10.1021/je960216+)
46. G. Ritzoulis, *Can. J. Chem.* **67** (1989) 1105 (<https://doi.org/10.1139/v89-166>)
47. M. A. Saleh, O. Ahmed, M. S. Ahmed, *J. Mol. Liq.* **115** (2004) 41 (<https://doi.org/10.1016/j.molliq.2003.12.021>)
48. S. B. Aznarez, L. Mussari, M. A. Postigo, *J. Chem. Eng. Data* **38** (1993) 270 (<https://doi.org/10.1021/je00010a022>)
49. S. Parveen, D. Shukla, S. Singh, K. P. Singh, M. Gupta, J. P. Shukla, *Appl. Acoust.* **70** (2009) 507 (<https://doi.org/10.1016/j.apacoust.2008.05.008>)
50. B. Nagarjun, A. V. Sarma, G. R. Rao, C. Rambabu, *J. Thermodyn.* **2013** (2013) 285796 (<https://doi.org/10.1155/2013/285796>)
51. A. Zhu, J. Wang, R. Liu, *J. Chem. Thermodyn.* **43** (2011) 796 (<https://doi.org/10.1016/j.jct.2010.12.027>)
52. A. Ali, A. K. Nain, V. K. Sharma, S. Ahmad, *Phys. Chem. Liq.* **42** (2004) 375 (<https://doi.org/10.1080/00319100410001679882>)
53. P. R. Bevington, D. K. Robinson, *Data reduction and error analysis for the physical sciences*, McGraw-Hill, New York, 1969, pp. 235–242 (ISBN 0-07-247227-8)
54. M. Dhiman, K. Singh, D. P. Gupta, D. P. Singh, A. Upmanyu, *Study of excess acoustical and thermo-dynamical parameters of binary solutions of polypropylene glycol-400 and n-alkanols at 303 K*, AIP Conf. Proc., AIP Publishing, Melville, NY, 2020 (<https://doi.org/10.1063/5.0001107>)
55. B. Thanuja, G. Nithya, C. C. Kanagam, *Ultrason. Sonochem.* **19** (2012) 1213 (<https://doi.org/10.1016/j.ultsonch.2012.03.006>)
56. A. Awasthi, A. Awasthi, *Phys. Chem. Liq.* **51** (2013) 112 (<https://doi.org/10.1080/00319104.2012.690569>)
57. G. V Rao, A. V. Sarma, D. Ramachandran, C. Rambabu, *Ind. J. Pure App. Phys.* **42** (2004) 820 (<http://nopr.niscpr.res.in/handle/123456789/8851>)
58. S. F. Babavali, D. Punyaseshudu, K. Narendra, C. S. Yesaswi, C. Srinivasu, *J. Mol. Liq.* **224** (2016) 47 (<https://doi.org/10.1016/j.molliq.2016.09.079>)
59. M. Dhiman, A. Upmanyu, P. Kumar, D. P. Singh, *Karbala Int. J. Mod. Sci.* **8** (2022) 703 (<https://doi.org/10.33640/2405-609X.3270>)
60. S. Gahlyan, M. Rani, S. Maken, *J. Mol. Liq.* **199** (2014) 42 (<https://doi.org/10.1016/j.molliq.2014.08.011>)
61. H. E. Hoga, R. B. Torres, *J. Chem. Thermodyn.* **43** (2011) 1104 (<https://doi.org/10.1016/j.jct.2011.02.018>).